

## ENGINEERING AND GINNING

### Apparatus and Infield Evaluations of a Prototype Machine Vision System for Cotton Plant Internode Length Measurement

Cheryl McCarthy\*, Nigel Hancock, and Steven Raine

#### ABSTRACT

**An on-the-go infield machine vision system was developed to measure internode length (i.e., the distance between main stem nodes) of cotton (*Gossypium hirsutum* L.) plants, which is a significant indicator of past water stress. An infield vehicle was developed to convey the machine vision system automatically across the crop canopy. This paper presents an evaluation of the devised system under a range of operational and field conditions. On average, the vision system's internode length detection rate ranged from 12 measurements per 100 plants for compact plants when the sun was directly overhead with respect to the camera, to 64 measurements per 100 plants for vigorous plants when the sunlight was perpendicular to the camera view angle. Imaging at night time using 850 nm near-infrared illumination resulted in internode length detection rates not significantly different from the most reliable daylight conditions. Both across-row and along-row operations of the system were evaluated, with the system yielding internode length measurements for groundspeeds up to 0.20 m/s for along-row operation. Visual occlusion of the main stem nodes by foliage and variations in natural lighting conditions were observed to be the principal reasons for internode lengths not being detected successfully for every plant. However, from the success rates observed, it is concluded that the system has the practical capability to map internode length across a field and hence, identify spatial trends in internode length from which trends in plant water stress can be inferred.**

**M**achine vision has potential application to crop monitoring tasks that are typically performed manually by humans based on visual assessment.

Measuring an adequately representative sample of plants within a field implies the acquisition of considerable quantities of data (McCarthy et al., 2010). Therefore, automation of crop sensing by machine vision offers potential benefits of labor savings and performance repeatability that is unaffected by human fatigue.

Crop sensing tasks that have been demonstrated using machine vision successfully in outdoor conditions are: automated identification of weed species (Slaughter et al., 2008), nitrogen status (Noh et al., 2005), plant size (Shrestha and Steward, 2005), and multispectral properties using narrowband imaging (Carter and Miller, 1994). A ground-based machine vision system might be deployed in the field on a regular basis, thus providing information about how a field is changing as well as measuring parts of the field relative to each other. For example, the sensing system could be mounted on an irrigation machine to identify infield differences as the machine performs a pass of the field (Sadler et al., 2002).

McCarthy et al. (2009) developed a machine vision system that used natural lighting and shape-based algorithms to identify cotton (*Gossypium hirsutum* L.) plant internode length. This was the first reported attempt to identify branching structure of plants in a row crop using machine vision and its application in determining irrigation requirement. Other potential uses of a machine vision system that automatically measures plant growth and development include ground truthing of remote sensing images and crop phenotyping. Spectral data from remote sensing images can be used to estimate plant growth and crop condition based on normalized vegetation difference index (Ritchie and Bednarz, 2005) and water stress based on thermal imagery for irrigation scheduling (DeTar et al., 2006). Hence, there is potential for the machine vision system to provide ground-based calibration information for these applications.

Cotton plants follow a structured growth and development pattern in which a new node develops on the main stem every 2 to 3 d. Internode length in cotton becomes fixed (i.e., ceases to elongate) below the fourth node (Fig. 1a). Morphological develop-

---

C. McCarthy\*, N. Hancock, and S. Raine, National Centre for Engineering in Agriculture, Faculty of Engineering and Surveying, University of Southern Queensland, West Street, Toowoomba Qld 4350, Australia

\*Corresponding author: cheryl.mccarthy@usq.edu.au

ment of the main stem of a cotton plant slows down when the plant's vegetative growth competes with boll development (Hearn, 1994). Hence, optimization of yield requires a balance between internode length and boll development.

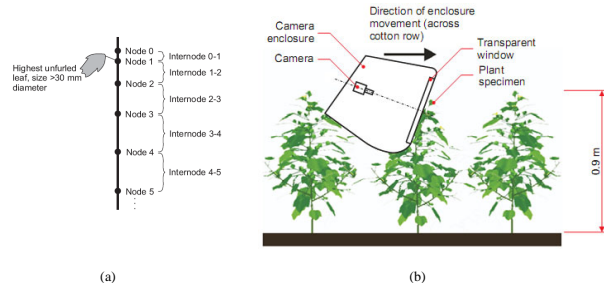


**Figure 1. Internode length measurement system: (a) diagram of cotton plant node numbering. Vertical black line represents the plant's main stem; and (b) moving image capture apparatus. Cotton plant graphic adapted from University of Hamburg (1998).**

Internode length measurement is part of plant-based water stress monitoring for cotton (Milroy et al., 2002) and can be used to quantify the effects of water and nutrient stress on main stem elongation rate (Landivar et al., 1996). Short internode lengths can result from water stress (Landivar et al., 1996), high fruit retention (Cothren et al., 1996), pest damage (Phipps et al., 1997), and exposure to cold temperatures (Livingston et al., 1998). Therefore, internode length on its own does not provide sufficient information to indicate water stress but can potentially be used in conjunction with other plant, soil, and weather data to inform crop management strategies.

Internode length measurements below the fourth node indicate past stresses (i.e., at least 8 to 12 d earlier). A fully developed internode should be greater than 50 mm (McKenzie, 1998), with smaller internode lengths indicating stress and internode lengths greater than 70 mm indicating excessive vegetative growth. The length of the higher internodes potentially indicate current main stem growth rate (Landivar et al., 1996). Automated internode length measurement has potential use both as an agronomic tool and in applications that require real-time input from sensors such as variable rate irrigation (Smith et al., 2009).

An infield internode length measurement system was developed by McCarthy et al. (2009) that consisted of a fiberglass camera enclosure (overall dimensions 520 mm × 290 mm × 520 mm) that continuously traversed the crop canopy (Fig. 1b). The camera enclosure made use of the flexible upper mainstem of the plants to first approach and then nondestructively contact and move over the plants. When the plant

contacted a transparent panel at the front of the camera enclosure, the transparent panel became a fixed object plane from which geometric measurements could be made. A video camera (Sony TRV-19E) mounted behind the transparent panel collected images of the plants as the camera enclosure traversed the canopy. An automatic image analysis algorithm that detected branches and their intersections with the main stem was developed to automatically measure internode length (McCarthy et al., 2009).

McCarthy et al. (2009) evaluated the system on a data set of 168 video sequences, each featuring one plant. They reported an overall detection rate of 57 measurements per 100 plants with standard errors ranging from 1.1 to 5.7 mm and an average of 3.0 mm, for an average internode length of 66.4 mm physically measured in the field. Detection rates varied from zero to three internode lengths per plant and overall, 11% of all internode distances were detected. McCarthy et al. (2009) reported that successful internode length detection in the image analysis was impeded by branches that were short, appeared bright, or were occluded by leaves.

It is envisioned that the machine vision system has potential use as an agronomic tool to measure internode length in real-time and with high spatial resolution in the field. Repeatable performance for different field and operational conditions is desirable for routine use of the vision system. The aim of this paper is to evaluate the system's repeatability under various conditions expected in a real-time field application, such as different times of day, cultivars, and row orientations. This necessitated development of an infield apparatus to convey the vision system in the crop for use in subsequent field evaluations.

## MATERIALS AND METHODS

**Prototype Infield Apparatus.** A four-wheeled chassis supporting a camera enclosure boom that spanned three cotton crop rows was designed and constructed to allow for automatic movement of the camera enclosure (Fig. 2a). It is anticipated that the camera enclosure can be mounted also on the boom of a center pivot or sprayer for both across- and along-row operations, or on a tractor for along-row operation.

Four degrees of freedom were required to adjust the camera enclosure's position and yaw angle during field measurements (Fig. 2b). "Traversal" was required to convey the camera enclosure across or along the crop rows. "Pitch" and "height" were adjusted so that the flexible upper main stem rested flat

against (i.e., parallel to) the front transparent panel and were typically held constant for a single set of canopy measurements. “Yaw” was the rotation about the enclosure’s vertical axis and was adjusted so that the camera always faced the plant it approached. Different yaw angles affected whether the plant curved under or sheared across the front of the camera enclosure and this effect was evaluated during field measurements.

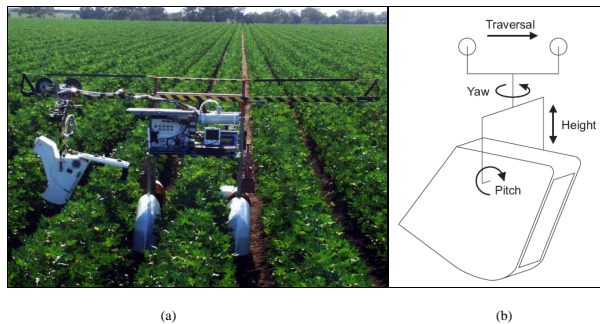


**Figure 2. Data collection apparatus: (a) infield vehicle for automated camera enclosure conveyance; and (b) required degrees of freedom for the camera enclosure.**

Windscreen wiper motors (12V) were used to motorize the traversal, yaw, and height adjustments as well as the chassis’ propulsion along the crop rows. The traversal movement was implemented using a pair of 200-mm trolley wheels that moved along a 50-mm steel channel (two lengths of angle steel welded together to make a U cross-section). Anti-skid tape (as commonly used on steps) was applied to the inner bottom surface of the boom rail to prevent the wheels from slipping. Worm drives on either side of the camera enclosure were used to adjust the camera enclosure’s height via two pulleys and a belt. The yaw rotation was implemented with a bicycle chain. The propel motor was geared 4:1 using a standard 1/2-inch pitch bicycle chain and sprockets. The pitch joint was not motorized because

this adjustment was required only once per data collection session.

Operator control of the motors was implemented via a panel of electrical switches (manual motor control) or via software on a PICAXE-40X microcontroller (automatic motor control), with control signals input to H-bridge motor drivers (part number D200 rated at 12V 60A from www.tecel.com). The microcontroller implemented a sequence of commands to activate the motors such that the camera enclosure traversed across the boom, turned around, and then waited while the chassis advanced down the row for a set distance (typically a few meters). Further details of the implementation can be found in McCarthy (2009). The system was powered by a 12V car battery charged by a solar panel.

Natural sunlight was used for illumination of the machine vision system during daytime trials. Illumination for night trials comprised a light-emitting diode (LED) array mounted along the top and bottom edges of the camera enclosure window, with each array holding a row of 850 nm, 940 nm, and white LEDs (McCarthy, 2009).

**Field Trials to Evaluate Operational Constraints.** The machine vision system was used to collect video sequences of cotton plants during crop flowering of the 2005-2006 and 2006-2007 Australian cotton growing seasons, at farms near Leyburn, Queensland (27.9°S, 151.5°E) and Jondaryan, Queensland (27.5°S, 151.6°E), respectively. Three replications of video sequences were collected for each treatment. Data sets were collected on different days and different crops, under varying operational and environmental conditions (Data sets 1 to 5, Table 1) and varying agronomic conditions (Table 2). The data set of McCarthy et al. (2009) was further evaluated in this paper and is denoted Data Set 1.

**Table 1. Data sets and evaluations.**

Data set	Number of plants	Crop row direction	Time of day	Evaluation			Agronomic conditions
				Lighting	Camera enclosure (Fig. 3)		
					Travel speed	Yaw angles	
1	14	North- south	1400 h–1500 h	Natural daylight	0.30 m/s across row	0°, 45°, 180°, 225°	Table 2
2	16	East-west	1200 h–1300 h				
3	10	East-west	1330 h–1430 h	Natural daylight	0.30 m/s across row	0°, 180°	Table 2
4	10	East-west	0830 h–0930 h				
5	13	North- south	1500 h–1600 h	Natural daylight	0.10, 0.20, 0.25 and 0.30 m/s along 30 m of the row	270°	
			1500 h–1600 h	Natural daylight and white LEDs	0.30 m/s across row	0°, 180°	Table 2
			1800 h–1900 h	White, 850 and 940 nm LEDs	0.30 m/s across row	0°, 180°	

Table 2. Data sets and agronomic details.

Data set	Cultivar	Age <sup>z</sup>	Season	Date	%GC <sup>z</sup>	Mean plant measurements (mm)		Reported growth habit <sup>x</sup>
						Height	Internode length <sup>y</sup>	
1	Sicot 80B	10	2005–2006	8 February 2006	90	907	66.4	Vigorous
2	Sicot 289B	11	2005–2006	21 February 2006	80	753	39.3	Vigorous
3	Sicot 71B	9	2005–2006	30 January 2005	50	589	53.6	Vigorous
4	Deltapine 408B	9	2005–2006	30 January 2005	70	739	60.5	Compact
5	Sicot 60B	11	2006–2007	2 February 2007	65	592	29.9	Compact

<sup>z</sup> Age is in terms of weeks after planting and %GC denotes percent ground cover.

<sup>y</sup> Measured with a ruler in the field.

<sup>x</sup> From cotton variety guides published by CSD (2007) and Monsanto (2010).

Consistent performance for different row orientations and times of day is desirable for routine use of the vision system. Therefore, the vision system was evaluated for different camera enclosure yaw angles (Fig. 3) and different times of day (Data sets 1 to 4). Different yaw angles were evaluated to determine whether shearing or bending of the plant's main stem produced significantly different results (Data Set 1).

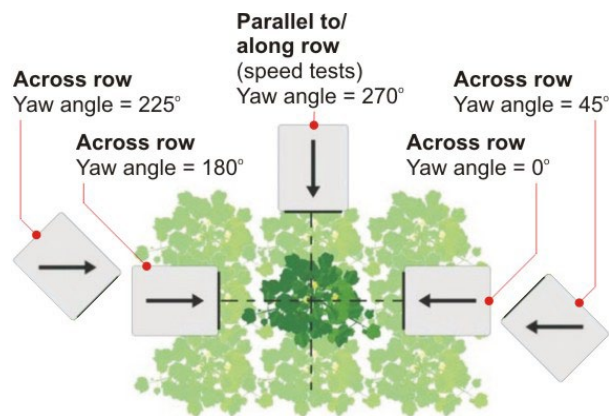


Figure 3. Camera enclosure yaw angle tests represented in plan view. The shaded grey rectangle depicts the camera enclosure. Cotton plant graphic adapted from University of Hamburg (1998).

A polar plot of the sun's position relative to the camera view angle for each data set is included in Fig. 4, based on the convention of Ranson et al. (1985) and using solar angle calculations from PVEducation (2010). The line segments labelled 1 to 5 represent the solar trajectory relative to the camera view angle for the data collection times of Data sets 1 to 5 in Table 1, a single quote after the number represents a yaw angle of 0° and numbers without a single quote represent a yaw angle of 180°. The distance of the line segments from the origin ( $\theta_s$ ) represents the sun's angular displacement

from directly above the camera enclosure (i.e., the solar zenith angle) and the angle  $\phi_{s/v}$  represents the horizontal angle through which the camera enclosure would have to turn to face the sun (i.e., the solar azimuth relative to the camera view angle).

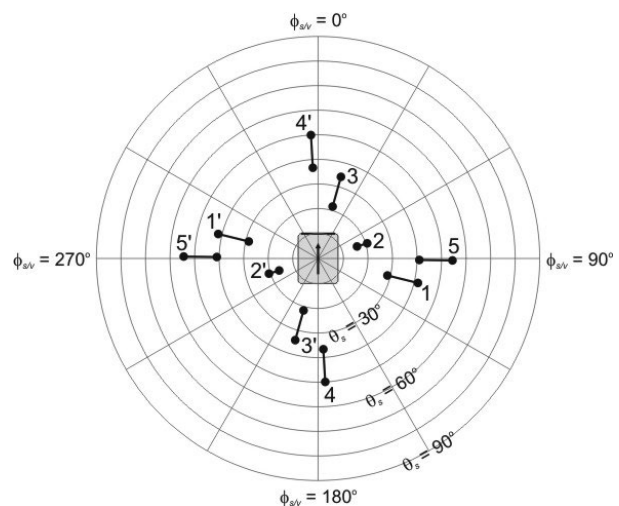
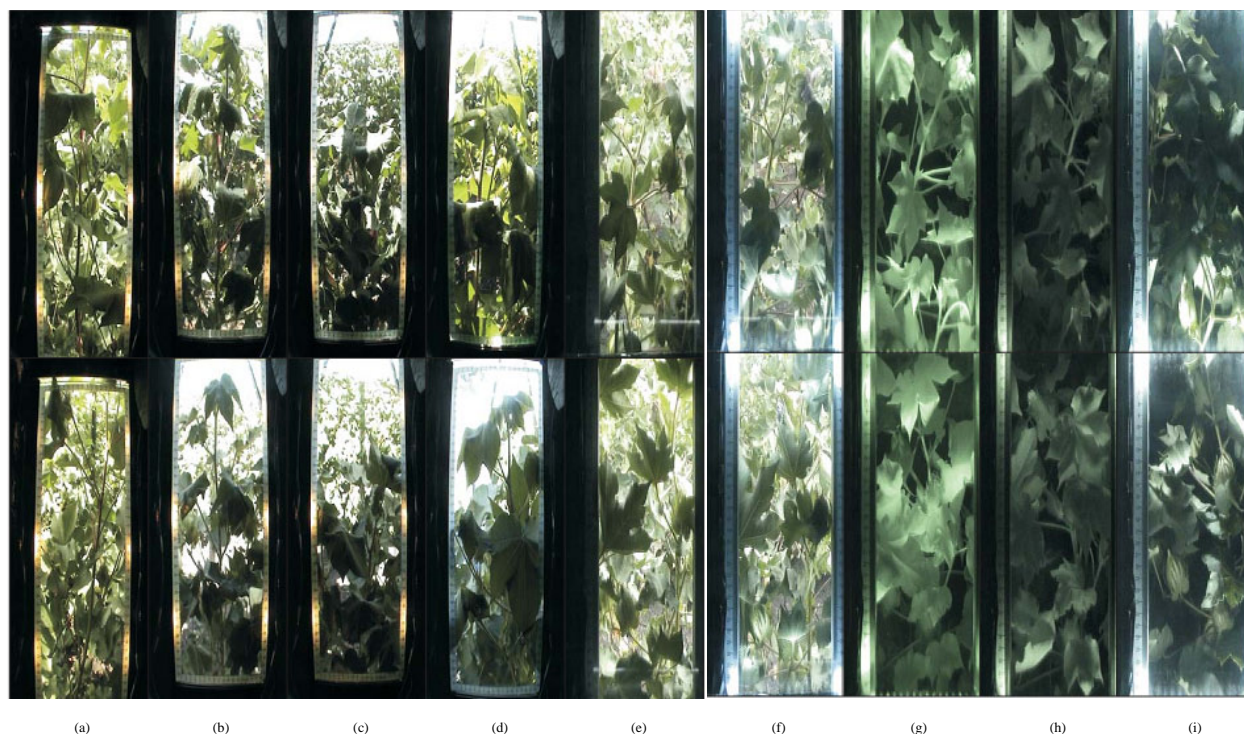


Figure 4. Polar plot representing the solar position relative to the camera's view angle during data collection of Data sets 1 to 5. See text for further description of the plot.

The system's operation at night with different light sources was also evaluated (Data Set 5). It is envisaged the system can operate across rows (e.g., mounted on a boom of an irrigation machine or sprayer) or parallel to rows (e.g., mounted on a tractor or quad bike). Therefore, operation both across and along rows was evaluated, with a range of speeds for tests parallel to the row to determine speed constraints for potential supporting machinery (Data Set 5). Agronomic conditions (crop cultivar and size) varied across data sets. Typical images for each data set are included in Fig. 5.



**Figure 5.** Typical images from the camera enclosure: (a)-(e) images from different times of day and night, representing Data sets 1 to 5 respectively; and (f)-(i) images of a single plant from Data Set 5, showing different lighting sources: (f) white LEDs in daylight; (g) 850 nm LEDs at night; (h) 940 nm LEDs at night; and (i) white LEDs at night. Top row: camera enclosure yaw angle of 0°; bottom row: camera enclosure yaw angle of 180°.

The results presented in McCarthy et al. (2009) indicated that variation was high in both detection rate (number of internode lengths measured per 100 plants) and measurement accuracy (absolute error in the internode length measurement) between replications of video sequences of individual plants in Data Set 1. The accuracy of the measurement was considered in Data Set 1 to determine the effect of shearing motion rather than bending motion of the plant associated with varying camera enclosure yaw angles. Only the number of internode length measurements obtained was considered for each other treatment. Statistical analysis was by ANOVA (Gomez and Gomez, 1984) using Microsoft Excel 2000 (Microsoft Corporation, Redmond, WA).

The top five internode lengths were physically measured with a ruler in the field for each plant imaged by the vision system to evaluate the vision system's performance. The "mean per 100 plants" for the number of internode lengths in the following evaluations (Tables 4 to 6) are with respect to a maximum of five internode lengths per plant.

**Image Analysis for Night Time Images.** Image analysis of the night time images followed the

process described in McCarthy et al. (2009) for daytime images but with additional preprocessing steps to invert the image intensity and adjust the image contrast (Fig. 6). This was required because the original algorithm only detected dark branches (McCarthy et al., 2009), whereas at night, illuminated branches appeared brighter than the background. The additional preprocessing steps were verified by visual observation to adequately detect branches at night time (Fig. 6).

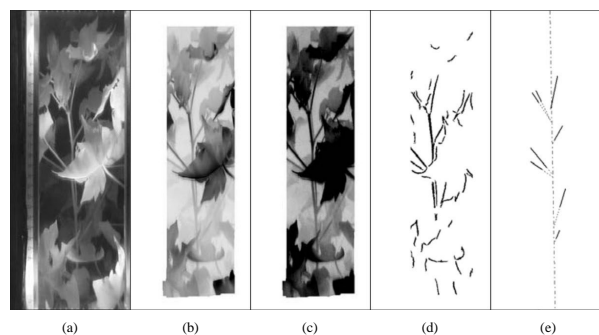


**Figure 6.** Image analysis for night time images (here, illuminated with 850 nm LEDs): (a) input image; (b) image region of interest with intensity inverted; (c) contrast stretching; (d) detected lines; and (e) straight lines representing main stem and candidate branches. Further details for steps (d) and (e) can be found in McCarthy et al. (2009).

## RESULTS AND DISCUSSION

**Camera Enclosure Yaw Angle Versus Internode Position.** In Data Set 1, three replications of video data were collected for each plant with camera enclosure yaw angles of 0, 45, 180, and 225° (Fig. 3). Mean absolute errors of internode length measurement for the different camera enclosure yaw angles and internode positions are presented in Table 3. Not all treatments and replicates identified each internode length. The missing data in Table 3 prevented an analysis of variance for interaction effects between all camera enclosure yaw angles and internode positions. However, an analysis of variance for all camera enclosure yaw angle treatments of Internode 2-3 and for three of the camera enclosure yaw angle treatments for Internodes 2-3 and 3-4 revealed no significant differences ( $P \leq 0.05$ ) in mean absolute error in internode length measurements between treatments. Hence, the measurement system did not yield significantly different accuracies for the shearing and bending motions of the camera enclosure over the plant.

**Table 3. Mean absolute errors in internode lengths in Data Set 1 for different camera enclosure yaw angles (Figure 3) and different internode positions for Data Set 1, with three replications.**

Internode position	Replicate	Mean absolute error in internode lengths (mm) for camera enclosure yaw angles across the row			
		0°	180°	45°	225°
Internode 0-1	I	4.00	11.90	-	-
	II	-	4.55	-	-
	III	-	-	-	-
Internode 1-2	I	1.20	6.83	5.20	13.07
	II	13.40	-	11.20	3.00
	III	7.40	1.80	-	-
Internode 2-3	I	7.13	8.95	7.20	10.70
	II	4.30	13.83	7.50	2.93
	III	6.20	4.50	2.60	2.00
Internode 3-4	I	7.00	-	5.47	3.17
	II	8.74	11.40	2.95	4.37
	III	6.68	-	5.25	8.20
Internode 4-5	I	2.37	-	9.70	4.55
	II	19.60	7.10	7.90	0.40
	III	-	-	13.40	-

The number of internode length measurements obtained for each camera enclosure yaw angle and internode position is presented in Table 4. An analysis of variance on this data found a significant ( $P \leq 0.05$ ) difference in the number of internode lengths detected with respect to different internode positions (i.e., Internode 0-1, 1-2, ..., 4-5; Fig. 1a). There was no interaction between the number of internode lengths detected and camera enclosure yaw angle for Internodes 0-1, 1-2, and 4-5. However, camera enclosure yaw angle did impact the number of measurements detected at Internodes 2-3 and 3-4, with fewer measurements occurring for the shear treatments. This was caused by the plant sliding past, rather than pushing against, the camera enclosure for the shear treatments, so the plant was in-frame for less of the video sequence. The camera enclosure yaw angles of 0° and 180° treatments were observed to have approximately equivalent areas of shadow and overexposure in images (Fig. 5a). However, Internode 3-4 was detected significantly less frequently for the yaw angle of 180° than for the yaw angle of 0°. This was due to repeated main stem occlusions caused by random arrangement of foliage, as verified by visual observation of images.

Comparison of the mean number of internode lengths detected per plant (Table 4) showed that the most commonly detected internode positions were Internodes 2-3 and 3-4, with detection rates of 21 and 15 internode length measurements per 100 plants, respectively. Five internode lengths were manually measured per plant so an automated detection rate of less than one measurement per plant is a low proportion. McCarthy et al. (2009) reported that the image analysis algorithm did not reliably detect branches that were short, bright, or occluded by leaves, which caused an overall low node detection rate, and that further algorithm development would be required to overcome these limitations. However, the machine vision system's ability to image plants on-the-go and in real-time indicated that a large data set might be collected if a large area of the field is imaged, even if individual plants cannot be identified and tracked (McCarthy et al., 2009). Practically, the detection rates for Internodes 2-3 and 3-4 indicate that on average, one Internode 2-3 measurement could be obtained every  $(100/21=)$  4.8 plants and one Internode 3-4 measurement could be obtained for every  $(100/15=)$  6.7 plants.

**Table 4. Number of internode lengths detected in Data Set 1 for different camera enclosure yaw angles (Fig.3) and different internode positions, with three replications.**

Internode position	Replicate	Number of internode lengths for camera enclosure yaw angles across the row <sup>z</sup>				Mean per 100 plants <sup>y</sup>
		0°	180°	45°	225°	
Internode 0-1	I	1	1	0	0	2 <sup>c</sup>
	II	0	2	0	0	
	III	0	0	0	0	
	Mean	0.33 <sup>A</sup>	1.00 <sup>A</sup>	0.00 <sup>A</sup>	0.00 <sup>A</sup>	
Internode 1-2	I	1	4	2	2	9 <sup>b</sup>
	II	1	0	1	1	
	III	1	2	0	0	
	Mean	1.00 <sup>A</sup>	2.00 <sup>A</sup>	1.00 <sup>A</sup>	1.00 <sup>A</sup>	
Internode 2-3	I	6	2	3	1	21 <sup>a</sup>
	II	4	4	4	3	
	III	2	5	1	1	
	Mean	4.00 <sup>A</sup>	3.67 <sup>AB</sup>	2.67 <sup>AB</sup>	1.67 <sup>B</sup>	
Internode 3-4	I	2	0	3	3	15 <sup>ab</sup>
	II	6	1	2	2	
	III	3	0	2	1	
	Mean	3.67 <sup>A</sup>	0.33 <sup>B</sup>	2.33 <sup>BC</sup>	2.00 <sup>C</sup>	
Internode 4-5	I	3	0	2	2	9 <sup>bc</sup>
	II	1	2	2	2	
	III	0	0	1	0	
	Mean	1.33 <sup>A</sup>	0.67 <sup>A</sup>	1.67 <sup>A</sup>	1.33 <sup>A</sup>	

<sup>z</sup> Upper case superscripts indicate significant differences across columns at the 1% level of significance.

<sup>y</sup> Averaged across four camera enclosure yaw angles, three replications and 14 plants.

Lower case superscripts indicate significant differences across rows at the 1% level of significance.

By inspection of analyzed images, Internodes 2-3 and 3-4 were commonly adjoined by long petioles (i.e., leaf stems) or branches that were readily detected by the image analysis algorithms. At the other end of the scale, the least-detected internode positions were Internodes 0-1 and 4-5. By inspection of analyzed images, Internode 0-1 was frequently occluded by the node's adjoining leaf because the node's petiole was comparatively short and the adjoining leaf was physically closer to the main stem. Node 5 commonly fell out-of-frame, which precluded Internode 4-5 from being automatically measured. A different camera enclosure design would be required to enable lower within-canopy movement to view the lower internodes, because of the more rigid branching structure closer to the ground.

**Illumination – Day Versus Night.** Data Set 5 consisted of video collected in daylight with and without artificial lighting, and at night with white and near-infrared (850 and 940 nm) lighting. The number and position of internode lengths detected for different lighting conditions are included in

Table 5. An analysis of variation showed there was a significant difference in the number of internode lengths detected with respect to different lighting conditions, but there was no interaction between lighting conditions and camera enclosure yaw angle. Natural daylight and 850 nm night time illumination yielded the most number of measurements (Table 5).

The number of internode lengths detected at 940 nm and with white LEDs, day or night, were not significantly different. The white LED illumination was not as effective at producing internode length results at night time as the 850 nm illumination. By inspection of analyzed images, the white LED illumination did not produce uniform illumination of the plant in front of the camera enclosure, due to leaves casting shadows on branches. The 850 nm illumination was more effective at illuminating the plant in front of the transparent panel with high contrast from the background. The 940 nm imagery had lower contrast than the 850 nm imagery. This was most likely due to the lower image sensor spectral sensitivity at the higher wavelength.

**Table 5.** Number of internode lengths detected in Data Set 5 for different lighting conditions and camera enclosure yaw angles at day and night, with three replications.

Light source at day/night	Replicate	Number of internode lengths for camera enclosure yaw angles across the row		Mean per 100 plants <sup>z</sup>
		0°	180°	
Natural light (day)	I	7	1	27 <sup>ab</sup>
	II	2	5	
	III	4	2	
	Mean	4.33	2.67	
White LED (day)	I	1	1	13 <sup>b</sup>
	II	1	2	
	III	2	3	
	Mean	1.33	2.00	
White LED (night)	I	1	2	12 <sup>b</sup>
	II	3	1	
	III	2	0	
	Mean	2.00	1.00	
850 nm LED (night)	I	2	5	38 <sup>a</sup>
	II	5	3	
	III	6	9	
	Mean	4.33	5.67	
940 nm LED (night)	I	1	1	15 <sup>b</sup>
	II	2	2	
	III	2	4	
	Mean	1.67	2.33	

<sup>z</sup> Averaged across two camera enclosure yaw angles, three replications and 13 plants.

Superscripts indicate significant differences across rows at the 10% level of significance.

#### Illumination – Shadow and Sun Angle Effects.

The vision system was used on five cotton cultivars to determine whether the crop cultivar caused significant differences in measurement system performance. However, variation of time of day and crop row direction affected this evaluation, because the cotton rows of Data sets 1 and 5 were oriented east-west, and north-south for Data sets 2 to 4 (Table 1). Fig. 4 indicates the sun's position relative to the camera view angle for each data set. The camera was either facing or turned away from the sun in Data sets 3 and 4, whereas in Data sets 1 and 5 the camera view angle was always perpendicular to the sunlight (solar azimuth angle). The sun was overhead of the camera (low zenith angle, Fig. 4) in Data Set 2. The average number of internode lengths detected for each data set is included in Table 6.

**Table 6.** Average number of internode lengths detected for different data sets (i.e., with different sunlight and agronomic conditions) and camera enclosure yaw angles with three replications.

Data set (%GC) <sup>z</sup>	Replicate	Number of internode lengths per 100 plants for camera enclosure yaw angles across the row <sup>y</sup>		Mean per 100 plants <sup>x</sup>
		0°	180°	
1 (90%)	I	50	93	64 <sup>a</sup>
	II	64	86	
	III	50	43	
	Mean	55	74	
2 (80%)	I	38	13	15 <sup>c</sup>
	II	13	6	
	III	13	6	
	Mean	21	8	
3 (50%)	I	40	10	12 <sup>c</sup>
	II	10	0	
	III	10	0	
	Mean	20	3	
4 (70%)	I	40	40	35 <sup>b</sup>
	II	10	50	
	III	10	60	
	Mean	20	50	
5 (65%)	I	8	54	27 <sup>b</sup>
	II	38	15	
	III	15	31	
	Mean	20	33	

<sup>z</sup>%GC denotes percent ground cover (from Table 2).

<sup>y</sup> Averaged across each data set's corresponding number of plants reported in Table 1.

<sup>x</sup> Averaged across two camera enclosure yaw angles and three replications.

Superscripts indicate significant differences across rows at the 5% level of significance.

Data Set 1 consisted of a camera enclosure view angle perpendicular to the solar azimuth angle and yielded the greatest number of internode length measurements. This was due to the reduced occurrence of dark shadowed areas and bright overexposed areas in images (McCarthy et al., 2009). Data sets 2 and 3 consisted of the lowest solar zenith angles of all the data sets evaluated and yielded the least number of internode length measurements (Table 6). The image background in these data sets consistently appeared overexposed compared to the foreground, regardless of the camera enclosure yaw angle (Figs. 5b and 5c).

Data sets 3 and 4 were captured with the sun behind or in front of the camera. Greater internode length detection rates when the sun was behind the camera (Table 6) because there were hard shadows along the length of the main stem and overexposed image backgrounds when the sun was in front of the camera enclosure (Fig. 5d, top). Internode length detection was less successful in sunlight conditions in which stem regions were frequently washed out by bright or overexposed background canopy (e.g. Figs. 5c to 5d). Overexposed backgrounds were observed to increase the brightness along branch edges, which reduced the apparent width of dark branches.

Plant edges on the transparent panel surface were more defined in Data sets 3 and 4 when the sun was behind the camera enclosure and the plant was in shadow (Fig. 5d, bottom). However, internode length detection rate was still low compared to the internode length detection rate of Data Set 1. This is believed to be because the cotton varieties tested were heliotropic, which caused the leaves to face the sun (and hence, the camera) rather than be randomly oriented. Internode length detection rate decreased as a result of more stem occlusions from the camera's view angle.

The variation in sunlight conditions prevented detailed conclusions being drawn about varietal differences in system performance. Under natural lighting conditions the best results were obtained with the camera view angle perpendicular to the solar azimuth angle.

**Crop Size and Cultivar.** The day/night evaluations demonstrated that the sunlight conditions of Data Set 5 did not degrade the system's performance compared to night time performance. However, Data Set 5 yielded significantly less internode length measurements than Data Set 1 (Table 6), yet both data sets were captured with the camera view angle perpendicular to the solar azimuth angle. Both data sets appeared to have visually similar image contrast (Figs. 5a and 5e). A possible explanation for the difference in performance was that the plants in Data Set 1 were physically larger than those in Data Set 5 (Table 6) and the image analysis algorithm was more reliable at detecting longer branches. For example, Data Set 5 consisted of a compact cultivar and a ground cover of 65%, whereas Data Set 1 consisted of a vigorous cultivar with an excessive vegetative growth habit and a ground cover of 90%.

Data Set 2 featured physically larger plants than Data Set 3 (Table 2). However, these data sets did not

perform significantly differently in terms of the number of internode lengths detected. In this case, the overexposed image background caused by overhead sunlight in Data Set 2 is believed to have reduced detection rate when compared to the lower angle of sunlight in Data Set 3. In comparison, Data sets 3 and 4 were captured under similar sunlight conditions yet Data Set 4 yielded more measurements. This is believed to be due to the plants in Data Set 4 being physically larger than the plants in Data Set 3 (70% versus 30% ground cover, Table 6).

**Camera Enclosure Travel Speed.** The effect of travel speed with the camera enclosure travelling parallel to the row direction (Fig. 3) was evaluated on Data Set 5 by calculating the mean absolute error and number of internode length measurements for different speeds (Table 7). The number of plants detected refers to the number of plants for those internode length measurements that were automatically detected. The range of speeds evaluated corresponded to expected speeds for various operation modes of the sensing system, i.e., on an irrigation machine or some other ground-based vehicle such as a tractor.

The machine vision system detected internode lengths for plants on an average of 3.3 m apart when travelling at 0.1 m/s (Table 7). This average distance between plants increased to 15 m at a camera enclosure travel speed of 0.25 m/s, and at 0.30 m/s the camera enclosure moved too fast to detect any internode length measurements. An analysis of variance showed that the travel speed of 0.25 m/s obtained significantly inferior results ( $P \leq 0.5$ ) to the other speeds. The image analysis algorithm of McCarthy et al. (2009) required a minimum of 10 sequential frames to detect a node. At 25 frames per second, this is equivalent to 0.4 seconds. However, the nodes were rarely detected for more than 10 sequential frames in images collected at 0.25 and 0.30 m/s.

Average plant spacing along a row is approximately 0.1 m so the maximum internode length detection rate is once per every 33rd plant, even at the slowest tested travel speed of the camera enclosure. Decreasing the camera enclosure travel speed further would be expected to increase the number of internode length measurements obtained by the automatic system. For example, the camera enclosure travel speed could be reduced to match the speed of a center pivot or lateral move tower (0.03-0.05 m/s), even for tractor-mounted operation.

**Table 7. Internode length results for different camera enclosure travel speeds along row for 30 m for Data Set 5.**

Speed along row (m/s)	Replicate	Number of plants detected	Average distance between detected plants (m)	Number of internode lengths detected	Mean absolute error (mm)
0.10	I	12	2.6	15	5.6
	II	11	2.8	12	6.1
	III	8	3.7	11	7.2
0.20	I	7	4.1	11	7.2
	II	8	3.4	13	8.9
	III	11	2.4	18	5.2
0.25	I	2	15.0	2	10.5
	II	2	15.0	2	9.4
	III	1	-	1	8.9
0.30	I	0	-	0	-
	II	0	-	0	-
	III	0	-	0	-

### PRACTICAL IMPLICATIONS OF SYSTEM PERFORMANCE.

*Physiological interpretation of measurements.* Typical grower monitoring involves measurement of the fourth-to-fifth internode distance, which is the top-most internode position that has ceased to elongate and indicates plant stresses 8 to 12 d earlier. The vision system most commonly detected the second and third internode distances, which are indicators of plant stresses from respective node initiations 4 to 9 d earlier up to the present (because the second and third internodes are still growing). Hence, the vision system potentially enables management decisions to be made about the second and third internode distances, which might influence and enable control of the future fourth-to-fifth internode distance. However, other crop conditions would be required to be known or sensed to interpret the cause of the plant stress.

*Natural lighting conditions during system use.* The most measurements were obtained for vigorous plants with the camera view angle perpendicular to the solar azimuth angle. Under these conditions the measurement rate was one internode length measurement per 1.77 plants (McCarthy et al., 2009). Sunlight perpendicular to the camera view angle yielded significantly more measurements than when the sun was in front or behind the camera. Heliotropic effects and overexposed image background reduced image quality when the sun was in front of or behind the camera, respectively. These environmental condi-

tions are restrictive to the routine use of the system during daytime and for particular crop row orientations. For example, irrigation machines can operate 24 h/d and the machine vision system mounted on the irrigation machine would vary in performance throughout the day.

The potential benefits of a shrouded camera enclosure should be evaluated. Alternatively, night time images captured with 850 nm LED illumination provided as many measurements as the corresponding daytime measurements. A benefit of night-time operation is that the effects of sunlight intensity variation and direction on system performance can be eliminated.

*Use of the system as a ground truthing tool for remote sensing images.* Average internode length detection rates per plant for the machine vision system were consistently less than one. Hence, measurements would not be obtained for all plants imaged. Practically this does not allow plants to be mapped in a single pass of the machine vision system or individually monitored over several measurement cycles. However, the system could be used to indicate spatial trends in internode length across a field. For example, internode length measurements obtained for an area of the field using the vision system might be used to calibrate a satellite or aerial image of the whole field, thus enabling conclusions to be drawn about water stress or plant growth across the whole field.

The internode length detection rates of 12 and 64 per 100 plants are equivalent to an average of one internode length measurement per  $(100/12 \times 0.9) = 7.5$

m and  $(100/64 \times 0.9 =) 1.4$  m, respectively, for a crop row spacing of 0.9 m. A camera enclosure travel speed of 0.5 m/s across the row would enable the camera enclosure to traverse a span of length 60 m of a lateral move irrigation machine in 200 s. The irrigation machine would advance 10 m in this time, assuming that the irrigation machine is travelling at a speed of 3 m/min. Hence, the system would detect  $(3 \times 30 / 7.5 =) 12$  to  $(3 \times 30 / 1.4 =) 64$  internode length measurements in a 30 m<sup>2</sup> area of the field. This would mean that for a Landsat TM satellite image with a spatial resolution of 30 m (Geoscience Australia, 2009), each pixel of the satellite image could be represented and ground truthed by 12 to 64 internode length measurements, depending on the agronomic and operational conditions in which the machine vision system was employed. It is anticipated that the suitability of the detection rate would need to be determined based on the specific sensing requirements for each application.

Along-row camera enclosure travel speeds up to 0.20 m/s yielded internode lengths using the current image analysis algorithms and hardware. Hence, the system might be used as a standalone agronomic tool, mounted off a tractor or quad bike and operating at maximum groundspeed of 0.20 m/s under the desired environmental conditions. Internode length data could be used to generate a map to inform crop management decisions.

## CONCLUSIONS

The feasibility for automated infield internode length measurement using a camera enclosure that is conveyed across the crop canopy was demonstrated. Automated conveyance of the camera enclosure across the plant rows was achieved using a four-wheeled chassis and four degrees of freedom on the camera enclosure's motion.

This study demonstrated a series of conditions that optimized the performance of the machine vision system. Further work on enhancing system robustness can be expected to enable operation of the system under a greater range of conditions. This might include optical and lighting design to emulate ideal conditions 24 h/d and adjusting the image analysis algorithm to detect a greater range of branch sizes.

The most reliable operation occurred on vigorous plants, with the camera view angle perpendicular to the solar azimuth angle and at night with infrared illumination. Hence, the current system would not

perform consistently for machines that operate 24 h/d. Rather, the system might be used as a tractor-mounted tool under the most reliable conditions of the camera view angle being perpendicular to solar azimuth angle or operating at night to measure cotton plant internode length. Detection rates were consistently less than one internode length per plant, so multiple plants would be required to be imaged in a field to generate a data set of measurements. Hence, the system would be suitable for indicating spatial trends in internode length measurement rather than monitoring of individual plants.

## ACKNOWLEDGMENTS

The authors are grateful to the Queensland cotton farms Macquarie Downs and Adelong for providing field trial sites and to agronomist Dr. Simon White for assistance in collecting field data. The senior author is grateful to the Cooperative Research Centre for Irrigation Futures ([www.irrigationfutures.org.au](http://www.irrigationfutures.org.au)) and the Australian Research Council for funding support.

## REFERENCES

- Carter, G., and R. Miller. 1994. Early detection of plant stress by digital imaging within narrow stress-sensitive wavebands, *Remote Sens. Environ.* 50:295–302.
- Cothren, J.T., J.A. Landivar, and D.M. Oosterhuis. 1996. Mid-flowering application of PGR-IV to enhance cotton maturity and yield. p. 1149. *In Proc. Beltwide Cotton Conf., Nashville, TN. 9-12 Jan. 1996. Natl. Cotton Council, Memphis, TN.*
- CSD (2007). Cotton Seed Distributors Variety Guide. Available at <http://www.csd.net.au> (verified 12 November 2010).
- DeTar, W.R., J.V. Penner, and H.A. Funk. 2006. Airborne remote sensing to detect plant water stress in full canopy cotton. *Trans. ASABE* 49(3):655–665.
- Geoscience Australia (2009). Satellite Facts. Available at <http://www.ga.gov.au/remote-sensing/satellites-sensors/satellite-facts.jsp> (verified 12 November 2010).
- Gomez, K., and A. Gomez. 1984. *Statistical Procedures for Agricultural Research*, John Wiley & Sons, New York, NY.
- Hearn, A.B. 1994. The principles of cotton water relations and their application in management. p. 66–92. *In G.A. Constable and N.W. Forrester (ed.) Challenging the Future. Proc. World Cotton Res. Conf. Brisbane, Australia. 14-17 Feb. 1994. CSIRO, Narrabri, NSW, Australia.*

- Landivar, J.A., J.T. Cothren, and S. Livingston. 1996. Development and evaluation of the average five internode length technique to determine time of mepiquat chloride application. p. 1153–1156. *In Proc. Beltwide Cotton Conf.*, Nashville, TN. 9-12 Jan. 1996. Natl. Cotton Counc. Am., Memphis, TN.
- Livingston, C.W., J.A. Landivar, and W.B. Prince. 1998. Effects of planting dates on fruit distribution and yield. p. 1503. *In Proc. Beltwide Cotton Conf.*, San Diego, CA. 5-9 Jan. 1998. Natl. Cotton Counc. Am., Memphis, TN.
- McCarthy, C.L. 2009. Automatic non-destructive dimensional measurement of cotton plants in real-time by machine vision. Ph.D. diss. Univ. of Southern Queensland, Toowoomba, QLD, Australia.
- McCarthy, C.L., N.H. Hancock, and S.R. Raine. 2009. Automated internode length measurement of cotton plants under field conditions. *Trans. ASABE* 52(6):2093–2103.
- McCarthy, C.L., N.H. Hancock, and S.R. Raine. 2010. Applied machine vision of plants – a review with implications for field deployment in automated farming operations. *Intell. Serv. Rob.* 3(4):209–217.
- McKenzie, D.C. (ed.) 1998. SOILpak for Cotton Growers. 3rd ed. NSW Agriculture, Orange, NSW, Australia.
- Milroy, S., P. Goyne, and D. Larsen. 2002. Cotton information sheet: irrigation scheduling of cotton, Tech.Rept., Australian Cotton Cooperative Research Centre.
- Monsanto (2010). Deltapine Products. Available at <https://www.deltapine.com> (verified 12 December 2010).
- Noh, H., Q. Zhang, S. Han, B. Shin, and D. Reum. 2005. Dynamic calibration and image segmentation methods for multispectral imaging crop nitrogen deficiency sensors. *Trans. ASAE* 48(1):393–401.
- Phipps, B.J., W.E. Stephens, J.N. Ward, T.V. Scales, and J.A. Wrather. 1997. The influence of in-furrow treatments upon early vigor and fiber quality of upland cotton. p. 1476–1481. *In Proc. Beltwide Cotton Conf.*, New Orleans, LA. 7-10 Jan. 1997. Natl. Cotton Counc. Am., Memphis, TN.
- PVEducation (2010), Sun Position Calculator. Available at <http://pvcdrum.pveducation.org/SUNLIGHT/SUN-CALC.HTM> (verified 12 November 2010).
- Ranson, K.J., C.S.T. Daughtry, L.L. Biehl, and M.E. Bauer. 1985. Sun-view angle effects on reflectance factors of corn canopies. *Remote Sens. Environ.* 18:147–161.
- Ritchie, G.L., and C.W. Bednarz. 2005. Estimating defoliation of two distinct cotton types using reflectance data. *J. Cotton Sci.* 9:182–188.
- Sadler, E.J., C.R. Camp, D.E. Evans, and J.A. Millen. 2002. Corn canopy temperatures measured with a moving infrared thermometer array. *Trans. ASAE* 45(3):581–591.
- Shrestha, D.S., and B.L. Steward. 2005. Shape and size analysis of corn plant canopies for plant population and spacing sensing. *Trans. ASAE* 21(2):295–303.
- Slaughter, D.C., D.K. Giles, and D. Downey. 2008. Autonomous robotic weed control systems: a review. *Comput. Electron. Agric.* 61:63–78.
- Smith, R.J., S.R. Raine, A.C. McCarthy, and N.H. Hancock. 2009. Managing spatial and temporal variability in irrigated agriculture through adaptive control. *Aust. J. Multidiscip. Eng.* 7(1):79–90.
- University of Hamburg (1998), Virtual Plants. Available at <http://www.biologie.uni-hamburg.de/b-online/virtual-plants/ipivp.html> (verified 12 December 2010).